Available online at www.sciencedirect.com
ScienceDirect
Journal of Power Sources 163 (2007) 1040–1046
JOURNAL OF POWER SOURCES
www.elsevier.com/locate/jpowsour

Synthesis and characterization of nanosized $LiNiVO_4$ electrode material

M.V. Reddy *, B. Pecquenard, P. Vinatier, A. Levasseur

ICMCB-CNRS/ENSCPB (CNRS UPR 9048), Université de Bordeaux 1, 33608 Pessac Cedex, France

Received 25 June 2006; received in revised form 21 September 2006; accepted 26 September 2006
Available online 13 November 2006

Abstract

Inverse spinel $LiNiVO_4$ thin films were prepared by rf-sputtering, fallowed by films annealed at 300, 450 and 600 °C for 2 h to induce the crystallization of the films. The films were characterized by X-ray diffraction, Rutherford backscattering spectroscopy, nuclear reaction analysis, Auger electron spectroscopy, atomic force microscopy and scanning electron microscope techniques. The Anodic electrochemical performance films have been cycled in the range of 0.02–3.0 V, at room temperature, at a current density 75 μA cm^{-2}. Galvanostatic cycling and cyclic voltammetry results shows characteristic cycling curves with respect to annealing temperature. The films annealed at 450 °C showed best electrochemical performance and excellent capacity retention during cycling was observed due to its nanosized morphology.

Keywords: $LiNiVO_4$ annealed films; Electrochemical properties; Anodes; rf-Sputtering; Rechargeable microbatteries

1. Introduction

Thin film lithium ion batteries are of potential importance in the area of low power applications such as micro-systems, micro-sensors, micromechanics, microelectronics and also implantable medical devices. The various cathodes, anodes and electrolytes materials for solid state rechargeable microbatteries have been studied [1–7]. Lithium metal was commonly used anode material for lithium microbatteries, it has several disadvantages like reactivity to moisture and safety problems. To overcome this problem to search for an alternative anode materials. In this aspect, recently $LiNiVO_4$ material showed promising negative electrode [6–13], because of its high specific capacity compared to graphite electrode. Reported literatures on nano-particles or nanostructured, thin films compounds showed a combination of rate capability, cycle life and electrochemical performance superior to that of electrode with bigger particle size [14–19]. Therefore, considering the aforementioned strategies, we report the simple method of preparation, analysis of nano sized to sub-micron $LiNiVO_4$ particles and electrochemical studies of the films.

2. Experimental

Lithium nickel vanadate films were prepared by using radio frequency (rf) sputtering technique and $LiNiVO_4$ was used as a target. The powder was prepared by solid state reaction of Li_2CO_3, NiO and V_2O_5, heated at 730 °C, 12 h in air. The pure argon (99.999%) and oxygen (99.99%) used as a carrier and reactive gas respectively, during sputtering. Before deposition of thin films, vacuum of $\sim 4 \times 10^{-5}$ Pa was applied into sputtering chamber. The deposition conditions of the thin films preparation are: a distance between target substrate of 8 cm, a power of 30 W, a partial pressure of oxygen (pO_2) of 10 mPa (1%), total working pressure of 1 Pa, and a substrates temperature about 50 °C (±5) during deposition. Whole sputtering unit was attached to an argon filled glove box to avoid contamination of films. The stainless steel (SS) substrates are used in electrochemical measurements, carbon or silicon (1 1 1) and aluminium foil (for thickness measurement) were used in RBS/NRA, SEM and AFM studies. The nano sized morphologies of the films are obtained by heating amorphous films from 300 to 800 °C for 2 h duration in a tubular furnace in an argon atmosphere. Annealed films with the thickness <1 μm are good adhesion to substrates.

The composition of thin films were examined by Rutherford Backscattering Spectroscopy (RBS), ($^4He^+$, 2 MeV) and the lithium concentrations are estimated by $^7Li(p\alpha)^4He$, Nuclear reaction Analysis (NRA). The homogeneity of thin films was carried out by using Auger electron spectroscopy (AES) (VG

* Corresponding author. Present address: Department of Physics, Solid State Ionics/Advanced Battery Lab, National University of Singapore (NUS), Singapore 117542, Singapore. Tel.: +65 65162605; fax: +65 67776126.
E-mail addresses: phymvvr@nus.edu.sg, reddymvv@hotmail.com (M.V. Reddy).

0378-7753/$ – see front matter © 2006 Elsevier B.V. All rights reserved.
doi:10.1016/j.jpowsour.2006.09.078

Micro lab 310 F). Crystal structure of powder and annealed films were identified by using the X-ray diffractometer (XRD) on Philips PW1730, equipped with Cu Kα radiation. Morphology of films was studied Scanning electron microscopy (SEM) (JEOL JSM-5200 microscope) and Atomic force microscope (AFM) (Dimension 3100, Digital instruments).

For electroanalytical studies like cyclic voltammetry (CV) and galvanostatic discharge–charge cycling, $LiNiVO_4$ film was used as working electrode and lithium metal foil as a counter and reference electrode. Polypropylene celgard membrane was used as a separator and presently preliminary electrochemical studies were performed with 1 M $LiPF_6$ (EC:DEC) (Merck) electrolyte. We note during preparation of thin film electrodes neither conducting carbon nor binder was used. Geometrical area of the electrode is 1.32 cm^2 and ~0.3 μm thick films are used to carry electrochemical measurements. The cells were fabricated in an Ar filled glove box. Galvanostatic discharge–charge cycling (constant current mode) and CV measurements were carried out at room temperature by using Bath lab battery tester and computer controlled VMP system (Bio-logic, France), respectively.

3. Results and discussion

3.1. Composition, structure and morphology aspects

The chemical composition of the films are obtained by using the Rutherford backscattering spectroscopy and nuclear reaction analysis are $Li_{1.1}NiVO_{4(\pm 0.1)}$ and the RBS spectra of the film was shown in the Fig. 1. Auger electro spectroscopy (AES) analysis showed atomic concentrations are homogeneous with the film thickness and more details on analysis of the films are reported elsewhere [11]. The Glancing-angle XRD patterns of as-deposited sputtered lithium nickel vanadate films are amorphous, this was also conformed by HRTEM images reported previously [12]. The XRD pattern of $LiNiVO_4$ target was shown in Fig. 2a. All peaks in the XRD patterns were indexed on the basis of inverse spinel structure assuming space group $Fd\bar{3}m$, where Li, Ni atoms occupy octahedral sites (16d) and V atoms are in tetrahedral site (8a) and O ions are 32e site. The compound shows a cubic lattice parameter value of $a = 8.219$ Å (JCPDS 38-1395). The XRD patterns of the films at various annealing temperature are shown in Fig. 2b. The continuous crystal growth of ($h\,k\,l$) lines is clearly seen with respect to annealing temperature (Fig. 2b). XRD pattern of annealed film show a major phase of $LiNiVO_4$ ($a = 8.22$ (7) Å) and small impurities of Li_3VO_4 or $LiVO_3$ phases (600 °C).

Fig. 3 displays the AFM topographic surface images and the corresponding three-dimensional plots of the annealed films. Film annealed at 450 °C (Fig. 3a) show a uniformly distributed grains with an average particle size is of order 20–40 nm. Whereas films annealed at 600 and 700 °C temperature, particle size varies from 70 to 90 nm and 110–150 nm, respectively (Fig. 3b and c). The observed result clearly shows the effect of annealing on $LiNiVO_4$ films induces the formation of larger grains. The corresponding three-dimensional (3D) plots (Fig. 3a'–c') of annealed films showed a root mean square (RMS) roughness varies from 10 to 25 nm. Also note that particle size, morphology and surface roughness play an important role in electrochemical performance [2,5,9,12–19]. TEM images of the annealed films on cupper grid was not studied due to experimental difficulties of the preparation films on TEM sample holder due to formation of Cu oxides above 300 °C [20]. Scanning electron microscopy (SEM) images of annealed films are shown in Fig. 4a and c, for comparison $LiNiVO_4$ powder prepared at same temperature by solid state method are also shown in the Fig. 4 b. The annealed thin films showed <80 nm

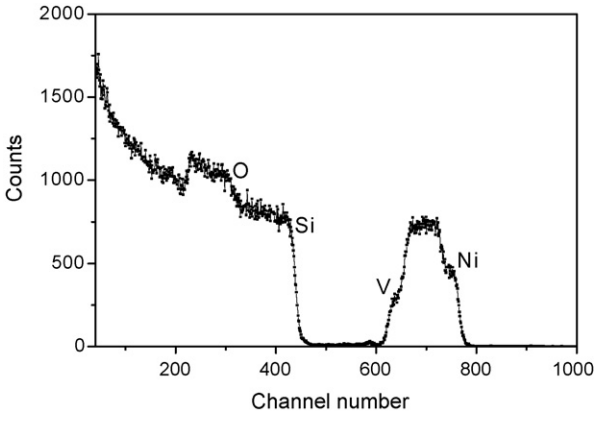

Fig. 1. RBS spectra of as-deposited $LiNiVO_4$ film on Silicon substrate, elements are shown in figure.

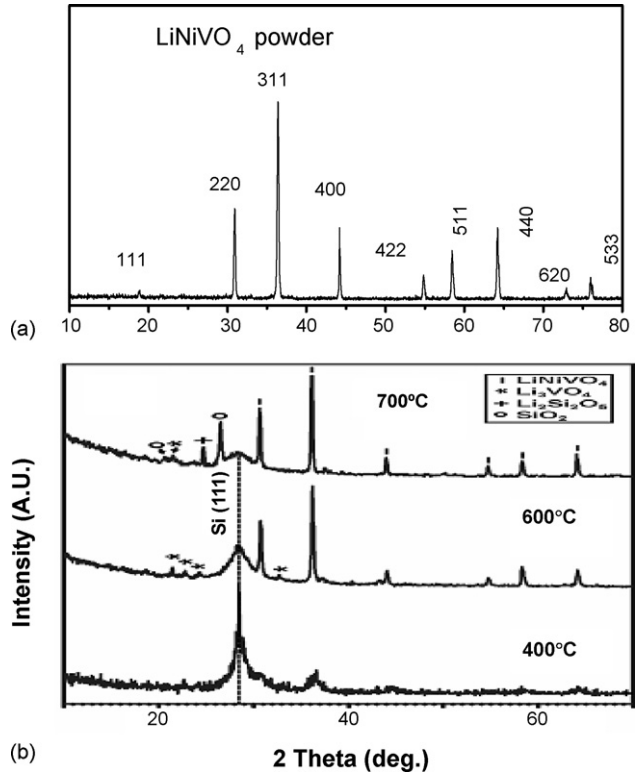

Fig. 2. X-ray diffraction pattern of $LiNiVO_4$ (a) powder (b) films annealed at 400, 600 and 700 °C; 2 h in argon atmosphere. Miller indices are shown in the pattern, with Cu Kα radiation. Thickness of film $t \sim 1$ μm, films deposited silicon (1 1 1) substrate.

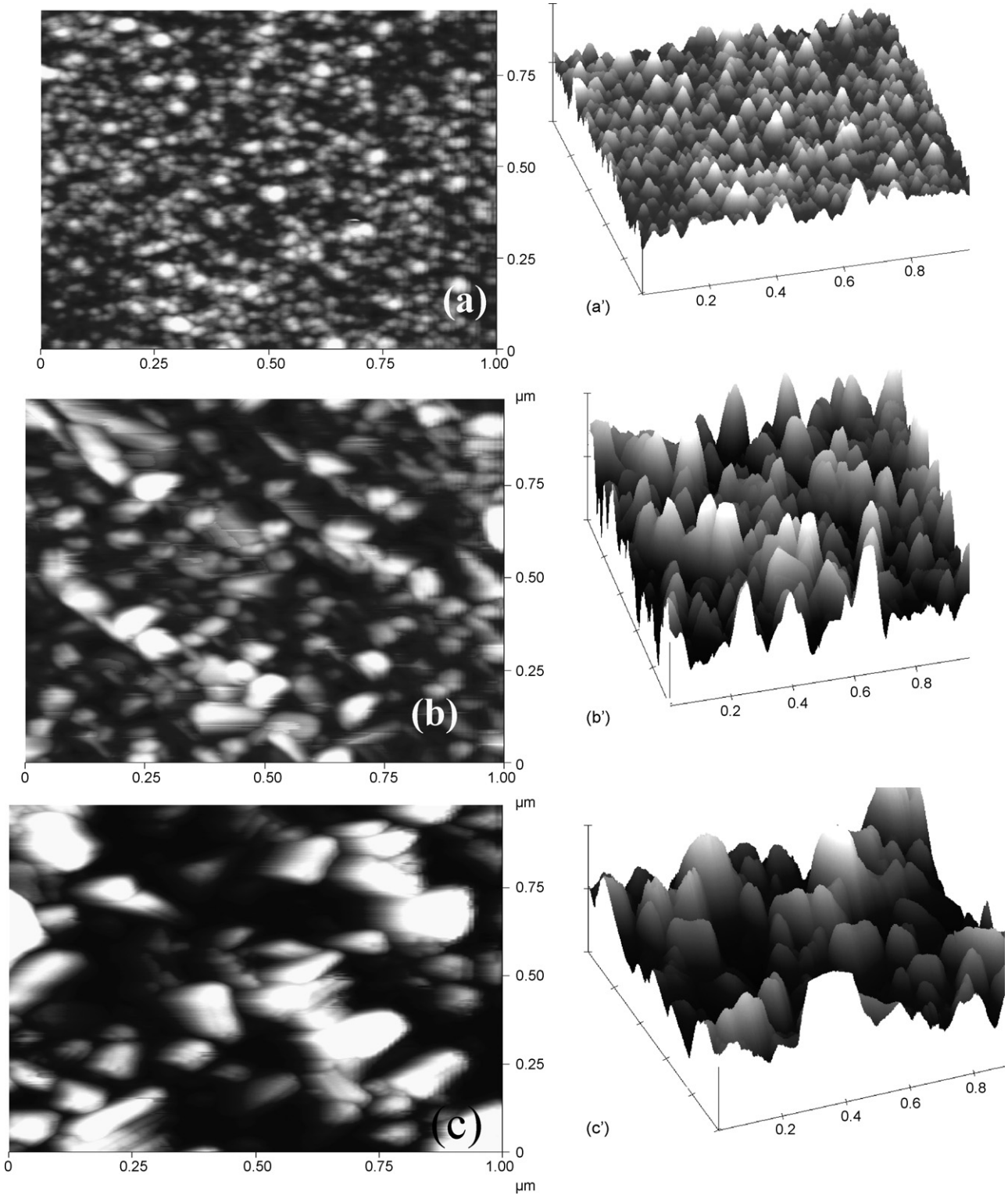

Fig. 3. Atomic force microscopy (AFM) images of $LiNiVO_4$ film, deposited on Silicon substrate, film thickness ~0.3 μm, annealed under Ar gas, for 2 h. (a) T: 450 °C. Bar scale, 1 μm × 1 μm; data scale, 10 nm. (b) T: 600 °C. Bar scale, 1.0 μm × 1.0 μm; data scale 20 nm, (c) T: 700 °C. Bar scale, 1.0 μm × 1.0 μm; data scale 20 nm. a'–c' are three-dimensional plots of a–c.

sized particles and $LiNiVO_4$ powder showed 6–10 μm sized, inhomogeneous particles (Fig. 4b). We also note that morphology of films can be controlled by varying growth conditions like annealing temperature, time of heating and thickness of the lithium nickel vanadate films (not discussed here).

3.2. Electrochemical measurements

The galvanostatic charge–discharge cycling of the $LiNiVO_4$ annealed film cells (300, 450 and 600 °C, 2 h) were carried out at room temperature, at a current density (j) 75 μA cm^2. The

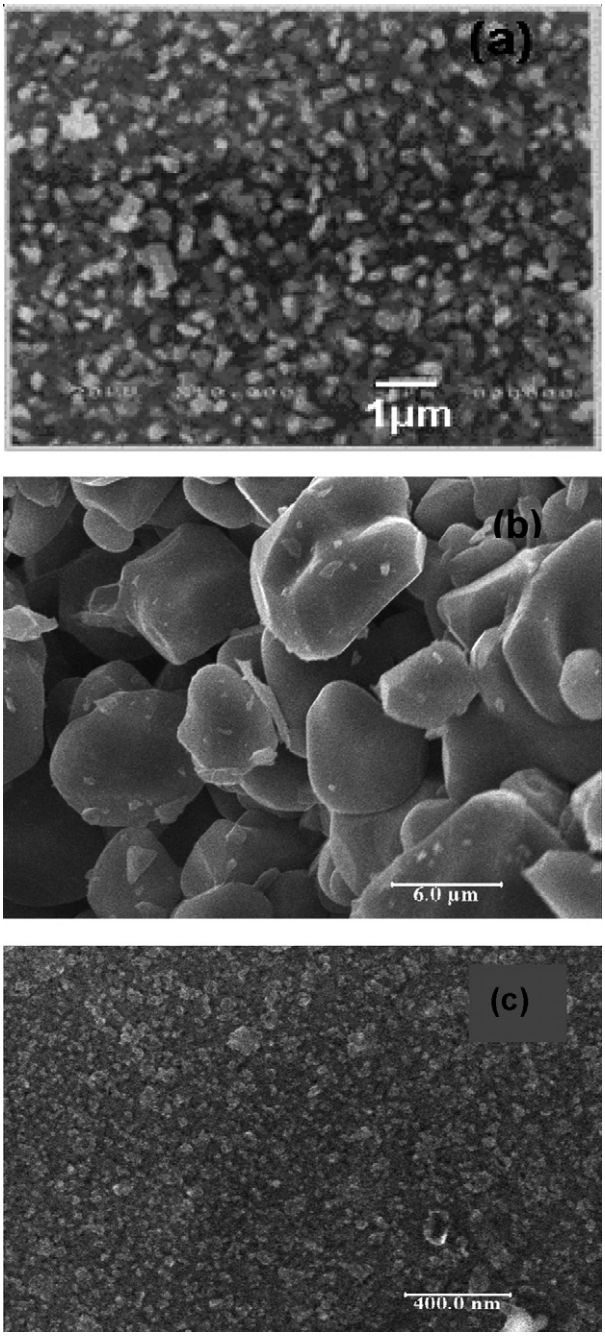

Fig. 4. SEM photo graphs of $LiNiVO_4$ (a) film annealed at 730 °C; Bar scale, 1 μm (b) bulk powder; Bar scale, 6 μm (c) film annealed at 600 °C; Bar scale 400 nm. Films deposited on silicon substrate and film thickness ∼0.3 μm.

cycling studies were carried out in the range of 3.0–0.02 V versus Li. The voltage versus number of lithium inserted into $LiNiVO_4$ films profiles are shown in Fig. 5a–c. During initial discharge process (lithium intercalation), the voltage suddenly decreased to ∼0.75–0.5 V with 1 mol lithium insertion in to the film form the open circuit voltage (∼3.0 V) after this, cell voltage decreases continuously till the lower cut-off voltage (Fig. 5a–c). In all the cases first charge cycle curves (lithium deintercalation) differs from those of first discharge curves (Fig. 5a–c). The irreversible capacity loss (ICL) during first discharge–charge cycle 1.1–1.8 Li, our observed ICL values are smaller compared to

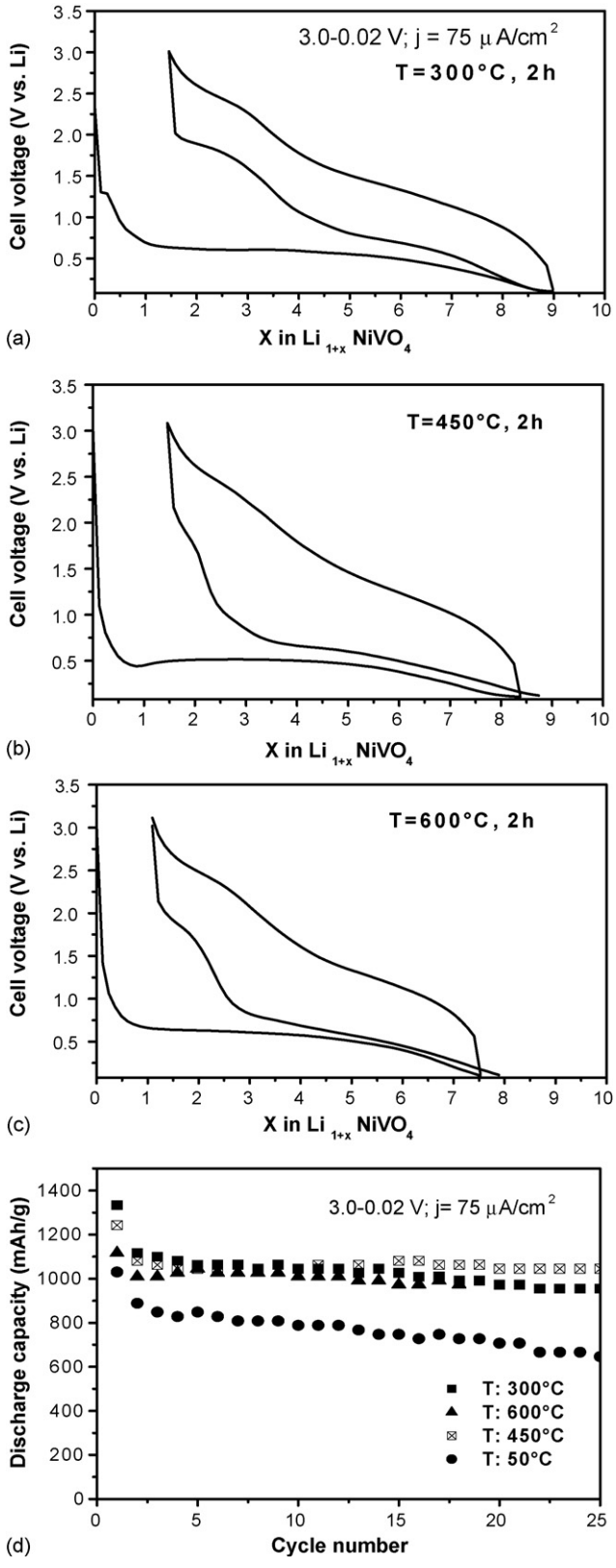

Fig. 5. (a) Galvanostatic discharge–charge cycling plots of annealed $LiNiVO_4$ films (voltage vs. number of lithium inserted) (a) 300 °C (b) 450 °C and (c) 600 °C. (d) Discharge capacity vs. cycle number. Voltage range: 3.0–0.02 V, current density $j = 75\ \mu A\ cm^{-2}$, and ∼0.3 μm, thick and geometrical electrode area 1.32 cm^2.

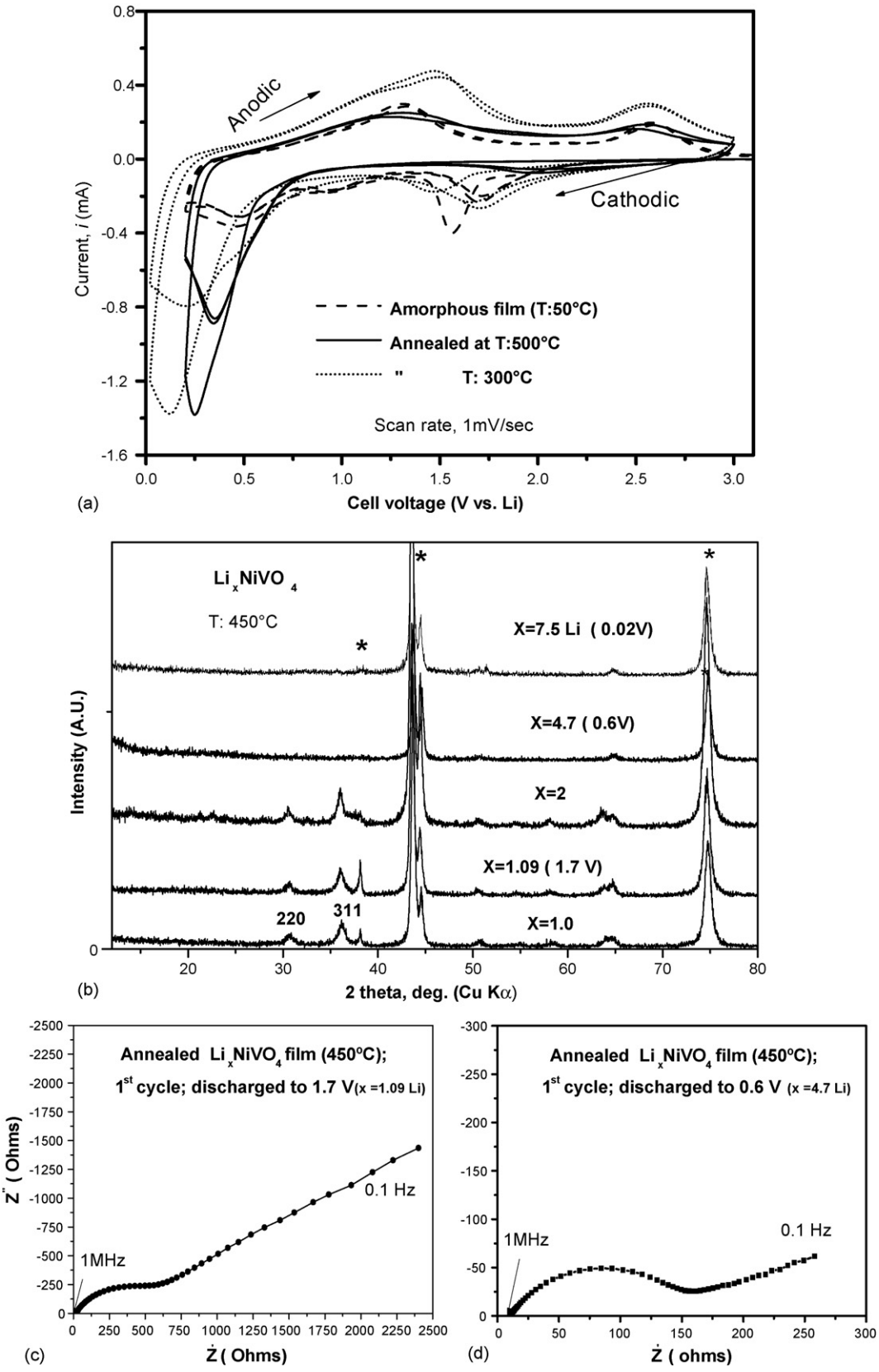

Fig. 6. (a) Cyclic voltammograms of $LiNiVO_4$ films recorded at a scan rate of 1 mV s^{-1}, annealed temperature shown in the Fig. 6a, 1 M $LiPF_6$ (EC:DEC) used as a electrolyte. Thickness film ~0.3 μm, Cycled in 3.0–0.02 V range. CVs recorded at ambient temperature, Li metal was the counter and reference electrode. Geometrical area of the electrode, 1.32 cm^2. (b) ex situ XRD patterns at various Li-insertion (x) into $LiNiVO_4$ films during first discharge cycle, film annealed at 450 °C, 24 h, thickness ~1.6 μm. The x values are shown in the XRD pattern and symbol (*) is stainless steel substrate peak. Impedance spectra of films annealed at 450 °C, thickness ~1.6 μm, 24 h vs. Li. (c) x = 1.08 Li (1.7 V) (d) x = 4.7 Li (0.6 V). Geometrical area of the electrode 1.32 cm^2.

that bulk $LiNiVO_4$ [8–10]. The discharge capacity versus cycle number up to 25 cycles was shown in the Fig. 5d. The 10^{th} discharge capacity values of annealed films was 1050 (±10) mA h g^{-1} (Fig. 5d), whereas amorphous film (T: 50 °C) showed slightly lower capacity and higher capacity fading compared to annealed films. Film annealed at 450 °C (2 h) show a excellent capacity retention during cycling, however bulk $LiNiVO_4$ material [8,9] showed higher capacity loss during electrochemical cycling. Similar improvement in the cycling performance of annealed films was reported previously in literature [5,16,17]. The improved electrochemical performance $LiNiVO_4$ material can be ascribed due to its nanocrystalline nature of the films and uniformly distributed grain particles during annealing.

Cyclic voltammetry (CV) (i–V) curves of annealed films and amorphous film are shown in Fig. 6a, CVs recorded at ambient temperature, at a scan rate of 1 mV s^{-1}. During first cathodic scan (lithium insertion) the voltammogram of amorphous film show a well resolved intense peak at 1.56 V, on further insertion of lithium a broad peak around ∼0.94 V, more intense peak at low voltage 0.46 V. While during first anodic scan (lithium deintercalation) a peak around ∼1.32 and ∼2.56 V are seen. Whereas annealed thin films show a peak voltages around ∼0.2–0.25 V during first cathodic scan and in anodic scan, peaks around ∼1.45 and ∼2.55 V. The voltammograms of amorphous film show characteristic nature, in this case Li-intercalation/deintercalation occurs in only one-step with a broad distribution of energy, whereas annealed films Li-intercalation occurs into $LiNiVO_4$ occurs in two-step mechanism or more depending on electrode particle size, this might be characteristic of nanosized or polycrystalline nature of the films. The redox mechanism and structural studies of bulk $LiNiVO_4$ by EXAFS and XANES [10] showed oxidation of nickel atom reduces to close to metallic state, where as vanadium oxidation state changes from 5 to 2. To study the crystal structure destruction of annealed $LiNiVO_4$ films during lithium intercalation, we carried out ex situ XRD studies of annealed films at 450 °C. After lithium insertion, cells were dismantled in a glove box, washed Li-inserted electrodes by using acetonitrile solvent and samples are fixed onto an air tight XRD holder along with stainless steel substrate. The ex situ XRD patterns with various Li-insertion amounts (x) are shown in the Fig. 6b. The XRD pattern are clearly show absence of *hkl* lines (2 2 0) and (3 1 1) at the end discharge (0.02 V; 7.5Li). This shows crystal structure destruction occurs after $x = 4.7$ Li inserted into $LiNiVO_4$ film, and amorphous at the end of the discharge. The preliminary electrochemical impedance spectroscopy (EIS) studies of annealed film (450 °C), on selected insertion amounts $x = 1.09$ Li and $x = 4.7$ Li, carried out at room temperature, the Nyquist plots (Z' versus $-Z''$) are shown in the Fig. 6c and d. Impedance spectra consists of a surface film resistance at a high frequency, middle frequency is due to charge transfer resistance (R_{ct}), it arises at the interface between the electrode and electrolyte and third semicircle at low frequency is the bulk resistance comes from the electronic resistivity of the active material and ionic conductivity in the pores of the electrode filled with the electrolyte [21,22]. The Nyquist plots clearly show the impedance values decreases depending on lithium insertion into $LiNiVO_4$ film, this is due to changes in the charge transfer resistance at the interface between the electrode and electrolyte [21,22], changes in oxidation states of metal ions and also structure destruction (seen from Fig. 6b). However we mention detail EIS studies on $LiNiVO_4$ films, at various voltages during discharge–charge cycle and different cycle number are needed to explain more detail electrode kinetics of the films.

4. Conclusions

We have demonstrated the preparation of $LiNiVO_4$ nano to submicron sized particles from the amorphous rf-sputtered $LiNiVO_4$ thin films. The films were characterized by RBS, NRA, AES and their crystal growth studied by XRD, SEM, and AFM. The electrochemical properties of annealed films were examined by cyclic voltammetry and charge–discharge cycling by using Li-metal as counter and reference electrode, with 0.02–3.0 V cut-off and at room temperature. CV shows characteristic (i–V) redox peaks with respect to annealed temperature. Charge–discharge cycling results of the $LiNiVO_4$ film annealed at 450 °C show a stable capacity of 1050(±10) mA h g^{-1}. Similar synthesis method by controlling growth conditions could be extended to preparation and characterization of other energy storage anodic metal oxides.

Acknowledgements

M. Lahaye, ICMCB-CNRS for help with AES and AFM.

References

[1] G. Meunier, R. Dormoy, A. Levasseur, Mater. Sci. Eng. B; Solid-State Mater. Adv. Technol. B3 (1989) 19.
[2] F.K. Shokoohi, J.M. Tarascon, B.J. Wilkens, Appl. Phys. Lett. 59 (1991) 1260.
[3] J.B. Bates, N.J. Dudney, B. Neudecker, B. Wang, New Trends Electrochem. Techn.: Energy Storage Syst. Electron. 453 (2000).
[4] I. Martin-Litas, P. Vinatier, A. Levasseur, J.C. Dupin, D. Gonbeau, F. Weill, Thin Solid Films 416 (2002) 1.
[5] E. Baba Ali, J.C. Bernède, D. Guyomard, Thin Solid Films 402 (2002) 215.
[6] S.J. Lee, H.-Y. Lee, T.-S. Ha, H.-K. Baik, S.-M. Lee, Electrochem. Solid State Lett. 5 (2002) A138.
[7] M.V. Reddy, C. Wannek, B. Pecquenard, P. Vinatier, A. Levasseur, J. Power Sources 119–121 (2003) 101.
[8] F. Orsini, E. Baudrin, S. Denis, L. Dupont, M. Touboul, D. Guyomard, Y. Piffard, J.-M. Tarascon, Solid State Ionics 107 (1998) 123.
[9] C. Rossignol, G. Ouvrard, J. Power Sources 97–98 (2001) 491.
[10] C. Rossignol, G. Ouvrard, E. Baudrin, J. Electrochem. Soc. 148 (2001) A869.
[11] M.V. Reddy, B. Pecquenard, P. Vinatier, C. Wannek, A. Levasseur, P. Moretto, Nucl. Instr. Meth. Phys. Res. B 246 (2006) 397.
[12] M.V. Reddy, B. Pecquenard, P. Vinatier, A. Levasseur, J. Phy. Chem. B 110 (2006) 4301.
[13] S.B. Tang, H. Xia, M.O. Lai, L. Lu, J. Electrochem. Soc. 153 (2006) A875.
[14] T. Brousse, R. Retoux, U. Herterich, D.M. Schleich, J. Electrochem. Soc. 145 (1998) 1.
[15] S.C. Nam, Y.H. Kim, W.I. Cho, B.W. Cho, H.S. Chun, K.S. Yun, Electrochem. Solid-State Lett. 2 (1999) 9.
[16] N. Li, C.R. Martin, B. Scrosati, Electrochem. Solid State Lett. 3 (2000) 316.
[17] N. Li, C.R. Martin, J. Electrochem. Soc. 148 (2001) A164.

[18] A.S. Arico, P.G. Bruce, B. Scrosati, J.-M. Tarascon, W.V. Schalkwijk, Nat. Mater. 4 (2005) 366.
[19] P.L. Taberna, S. Mitra, P. Poizot, P. Simon, J.-M. Tarascon, Nat. Mater. 5 (2006) 567.
[20] X. Jiang, T. Herricks, Y. Xia, Nano Lett. 2 (2002) 1333.
[21] N. Sharma, J. Plévert, G.V. Subba Rao, B.V.R. Chowdari, T.J. White, Chem. Mater. 17 (2005) 4700.
[22] M.V. Reddy, S. Madhavi, G.V. Subba Rao, B.V.R. Chowdari, J. Power Sources (2006), in press.